EuroIntervention 2015;10:1230-1238 published online ahead of print October 2014

Controlled circumferential renal sympathetic denervation with preservation of the renal arterial wall using intraluminal ultrasound: a next-generation approach for treating sympathetic overactivity

Kenichi Sakakura[1], MD; Austin Roth[2], MS; Elena Ladich[1], MD; Kai Shen[1], MD; Leslie Coleman[2], DVM; Michael Joner[1], MD; Renu Virmani[1]*, MD

1. CVPath Institute Inc., Gaithersburg, MD, USA; 2. ReCor Medical Inc., Palo Alto, CA, USA

This paper also includes accompanying supplementary data published online at: http://www.pcronline.com/eurointervention/81st_issue/204

KEYWORDS

- catheter
- pathology
- renal artery
- renal sympathetic denervation
- ultrasound

Abstract

Aims: The Paradise Ultrasound Renal Denervation System is a next-generation catheter-based device which was used to investigate whether the target ablation area can be controlled by changing ultrasound energy and duration to optimise nerve injury while preventing damage to the arterial wall.

Methods and results: Five ultrasound doses were tested in a thermal gel model. Catheter-based ultrasound denervation was performed in 15 swine (29 renal arteries) to evaluate five different doses *in vivo*, and animals were euthanised at seven days for histopathologic assessment. In the gel model, the peak temperature was highest in the low power-long duration (LP-LD) dose, followed by the mid-low power-mid duration (MLP-MD) dose and the mid-high power-short duration (MHP-SD) dose, and lowest in the mid power-short duration (MP-SD) dose and the high power-ultra short duration (HP-USD) dose. In the animal study, total ablation area was significantly greater in the LP-LD group, followed by the MLP-MD group, and it was least in the HP-USD, MP-SD and MHP-SD groups (p=0.02). Maximum distance was significantly greater in the LP-LD group, followed by the MLP-MD group, the MHP-SD group, and the HP-USD group, and shortest in the MP-SD group (p=0.007). The short spare distance was not different among the five groups (p=0.38). Renal artery damage was minimal, while preserving significant nerve damage in all groups.

Conclusions: The Paradise Ultrasound Renal Denervation System is a controllable system where total ablation area and depth of ablation can be optimised by changing ultrasound power and duration while sparing renal arterial tissue damage but allowing sufficient peri-arterial nerve damage.

**Corresponding author: CVPath Institute Inc., 19 Firstfield Road, Gaithersburg, MD, 20878, USA.*
E-mail: rvirmani@cvpath.org

SUBMITTED ON 15/04/2014 - REVISION RECEIVED ON 25/04/2014 - ACCEPTED ON 03/10/2014

DOI: 10.4244/EIJY14M10_14

EuroIntervention 2015;10:1230-1238

Introduction

Hypertension is strongly associated with cardiovascular morbidity and with mortality globally[1]. Despite the availability of multiple classes of antihypertensive medication, hypertension remains uncontrolled in a significant number of patients. Resistant hypertension is defined as blood pressure above goal despite the concurrent use of three different classes of antihypertensive medication, including one diuretic[2]. Chronic elevation in sympathetic activity contributes to the development of chronic hypertension, and potential end-organ damage[3]. Sympathetic nervous system overactivity has been linked to numerous pathophysiologic conditions affecting the renal, cardiovascular, and metabolic systems. Catheter-based renal denervation is a novel approach to disrupt renal sympathetic nerve activity in order to reduce blood pressure in patients with resistant hypertension[4] and other conditions related to sympathetic overactivity such as heart failure, obstructive sleep apnoea, chronic kidney disease, and diabetes[5,6].

To date, there are two primary approaches for catheter-based delivery of energy for renal denervation: 1) radiofrequency (RF) energy delivered to the renal arterial wall transmurally in order to ablate sympathetic nerves[7], and 2) ultrasound energy delivered circumferentially to the adventitia and periadventitia, sparing the arterial wall, to ablate the sympathetic nerves[8]. As compared to RF ablation, ultrasound ablation may have distinct advantages for renal denervation. First, the extent of thermal damage might be highly controllable both in the area and in the distance. Second, the renal arterial wall injury might be minimised since direct tissue contact is not necessary to deliver energy to the target tissue. The CE-marked Paradise® System (ReCor Medical Inc., Palo Alto, CA, USA) is a next-generation catheter-based device that has been designed to deliver ultrasound energy to perform targeted controlled circumferential denervation of renal sympathetic nerves. The aims of this study were: 1) to investigate whether modification of thermal tissue geometry is feasible by changing ultrasound doses (power and duration), and 2) to confirm the safety of renal arterial wall damage while ensuring ablation of periarterial nerves irrespective of different doses.

Methods

DEVICE OVERVIEW

The Paradise® System consists of a single-use 6 Fr ultrasound delivery catheter and an automated, portable customised generator **(Figure 1)**. The Paradise catheter consists of a through-lumen shaft with a cylindrical piezoelectric ceramic transducer located at the distal end of the catheter. The Paradise catheter has a distal balloon which is pressurised by the Paradise System in a range of 1.5-2.0 atm using sterile circulating water. The ultrasound transducer is located within the balloon. The transducer converts electrical energy to acoustic energy, which is then delivered radially from the balloon into the renal artery. The pressurised balloon centres the ultrasound transducer within the artery, and the circulation of fluid serves as coolant to protect the endothelial and medial layers of the renal arterial wall. Each catheter has an embedded chip which communicates directly with the Paradise generator to deliver the specific power settings to be applied. The Paradise generator contains a touch screen which allows the user to operate the Paradise System

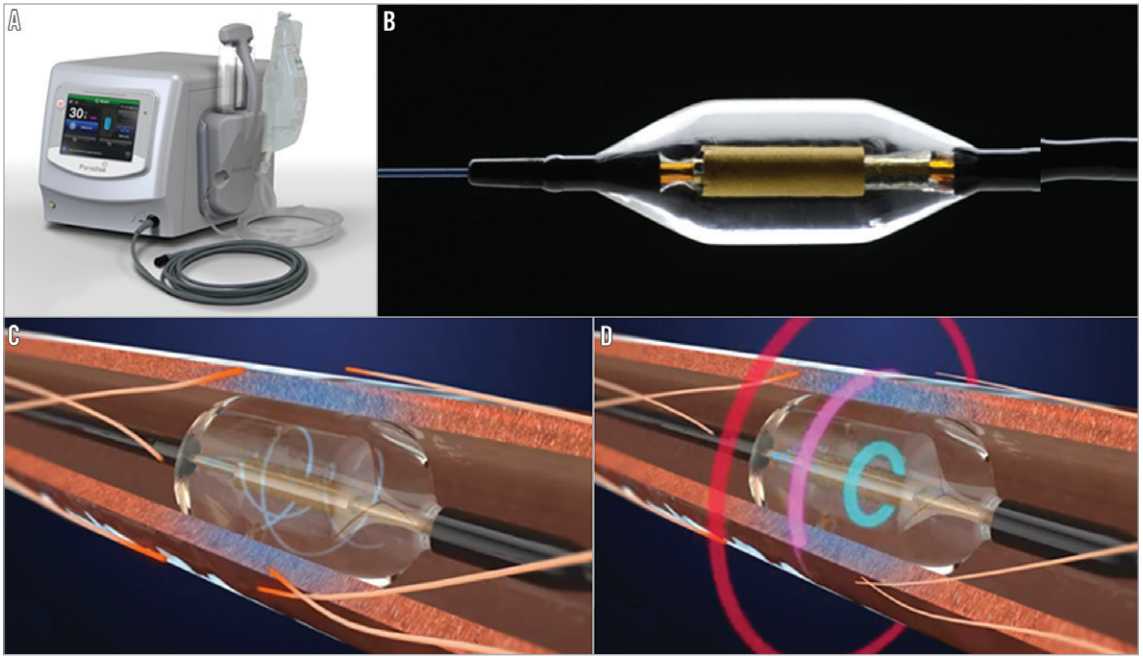

Figure 1. *Paradise Renal Denervation System. A) Paradise generator. B) Cylindrical transducer within a cooling balloon. C) Illustration of catheter within the artery demonstrating the cooling feature. D) Illustration of catheter within the artery demonstrating circumferential heating with concomitant balloon cooling.*

in a stepwise fashion to prepare the balloon for insertion, to inflate and/or deflate the balloon and to deliver ultrasound energy.

BENCH THERMAL GEL MODEL

A thermal gel model was utilised to predict the geometry of the tissue thermal lesion created following delivery of ultrasound energy. The gel model (HIFU Phantom Gel; Onda Corporation, Sunnyvale, CA, USA) is designed to mimic the thermal and acoustic properties of soft tissue. At body temperature (37°C) the gel is transparent; however, the gel becomes opaque at high temperatures (70°C), providing visual confirmation of lesion size and shape. A 5, 6, or 7 mm core is created in the centre of the gel to mimic an artery lumen. The appropriately sized balloon catheter is inserted into the gel ensuring circumferential balloon-gel contact, mimicking balloon-tissue contact. Temperature sensors are embedded in the gel at 1 mm and 5 mm to measure the actual temperature achieved during ultrasound sonication. Ultrasound energy was delivered per standard clinical use within the circulating cooling balloon. To characterise the controllability of ultrasound delivery, five different doses were tested in this model.

IN VIVO STUDY DESIGN

The safety and effectiveness of five selected ultrasound doses, based on bench gel data, were evaluated in a normotensive porcine model at ISIS Services, LLC (San Carlos, CA, USA). All procedures were in compliance with the USDA Regulations and the Animal Welfare Act (9 CFR Parts 1, 2 and 3), following the Guide for the Care and Use of Laboratory Animals[9]. The protocol for these studies was reviewed and approved by the Institutional Animal Care and Use Committee (IACUC) of the test facilities, which are accredited by the Association for Assessment and Accreditation of Laboratory Animal Care (AAALAC).

Fifteen Yorkshire cross swine, of both sexes, ranging from 62.5 to 83.5 kg were treated with two ultrasound emissions in each renal artery, and survived for seven days. Five different doses were used for the procedure. Three animals (6 RAs) were assigned to a low power and long duration dose, three animals (6 RAs) to a mid-low power and mid duration dose, five animals (10 RAs) to a mid power and short duration dose, two animals (4 RAs) to a mid-high power and short duration dose, and two animals (4 RAs) to a high power and an ultra-short duration dose. Each animal received the same test dose bilaterally.

RENAL DENERVATION PROCEDURE AND FOLLOW-UP

All animals were treated with aspirin (325 mg PO) and clopidogrel (75 mg PO) 24 hours prior to the procedure. Following general anaesthesia, a 7 Fr introducer sheath was placed via the femoral artery, and intravenous heparin administered to achieve an activated clotting time (ACT) of ≥300 seconds. Renal artery angiography was performed to determine the appropriate catheter size for treatment. The Paradise catheter was introduced and advanced via fluoroscopic guidance through a 7 Fr guide catheter over a 0.014" guidewire. The catheter was advanced to the target distal location. The balloon was inflated, ensuring full contact with the artery wall **(Figure 2)**. The calculated balloon/vessel ratio was 1.04. Ultrasound energy was delivered while the cooling fluid circulated through the balloon (cooling flow rate was 41 ml/min). Following completion of energy delivery, the balloon was deflated and the catheter re-positioned proximally for the second energy emission. Post procedure all animals were treated with aspirin (81 mg PO) and clopidogrel (75 mg PO) daily. At seven days, the animals were humanely euthanised. The renal arteries were perfused with lactated Ringer's solution followed by 10% neutral buffered formalin (NBF). The renal arteries, segment of aorta, and kidneys were fixed in 10% NBF and submitted to CVPath Institute, Inc., along with portions of psoas muscle, small intestine and ureter whenever a gross finding of discolouration and/or areas of necrosis were observed, for histologic examination.

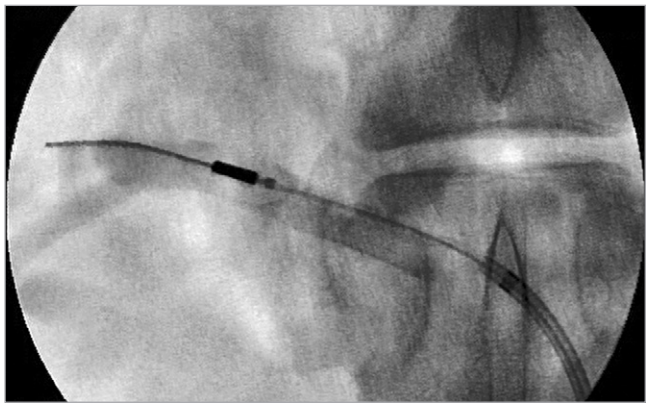

Figure 2. *Representative image of renal artery angiogram. The Paradise System was introduced through the guide catheter and positioned in the mid-distal renal artery.*

STANDARD HISTOPATHOLOGY

Renal arteries with surrounding tissue were cut into six to 11 sections (at 3-5 mm intervals) along the length of the artery, and submitted in separate cassettes for dehydration and paraffin embedding. Sections five microns thick were cut on a rotary microtome and stained with haematoxylin and eosin and modified Movat's Pentachrome. The renal artery, vein, arterioles, and renal nerves were assessed for injury using a semi-quantitative analysis scale of 0-4, wherein 0=none, 1=minimal, 2=mild, 3=moderate, and 4=marked injury[10].

Arterial and venous endothelium damage was circumferentially evaluated: 0=no endothelial loss, 1=endothelial loss <25% of vessel circumference, 2=endothelial loss 25-50% of vessel circumference, 3=endothelial loss 51-75% of vessel circumference, 4=endothelial loss >75% of vessel circumference[10]. Medial injury was evaluated both by the depth and by the circumference of involvement separately: 0=no medial change, grade 1=medial injury involving <25% of medial depth/circumference, grade 2=medial injury 25-50% of medial depth/circumference, grade 3=medial injury 51-75% of medial depth/circumference[10], and grade 4=medial injury >75% of medial depth/circumference. Nerve damage was given an

ordinal grading of 0 to 4: 0=none, 1=minimal, 2=mild, 3=moderate, and 4=severe, based on the histological extent of nerve injury[10]. Maximum nerve damage was recorded in each section.

In addition, to evaluate the extent of tissue damage circumferentially, the following parameters were evaluated: (1) number of quadrants with nerve fascicles; (2) number of quadrants with injured nerve fascicles (grade 2 or greater); (3) number of quadrants with moderately to severely injured nerve fascicles (grade 3 or greater); (4) number of quadrants with injured periarterial soft tissue.

MORPHOMETRIC ANALYSIS

Two emission sites (one from proximal and the other from distal) were determined in each renal artery. These two emission sites were used for the morphometric analysis. In the morphometric analysis, the area of the thermal ablation zone, the ablation zone "near field" distance (defined as the shortest distance between the arterial lumen and the ablation zone) and the ablation zone "far field" distance (defined as the longest distance between the arterial lumen and the ablation zone) were measured in each section **(Figure 3)**.

STATISTICAL ANALYSIS

Results were expressed as mean±SD. The mean score of two emission sites per each renal artery was used for analysis. Normality of distribution was tested with the Shapiro-Wilk test. Comparisons of variables with normal distribution were accomplished by one-way analysis of variance (one-way ANOVA), whereas comparisons of variables with skewed data distribution were performed by the Kruskal-Wallis test. A value of $p<0.05$ was considered statistically significant. All analyses were performed with SPSS software version 19 (IBM Corp., Armonk, NY, USA), and JMP 5 (SAS Institute, Cary, NC, USA).

Results

THERMAL PROFILE IN GEL MODELS

The optical feature of the thermal gel model demonstrated that the thermal lesion associated with delivery of ultrasound energy centred within a cooling balloon consists of a predictable and reproducible geometry characterised by a circumferential uniform toroidal lesion with a cooled zone adjacent to the balloon **(Figure 4)**. Embedded temperature sensors depict the controllability of the lesion as shown in **Table 1**. Peak temperature at 1 mm was similar among five doses (ranging from 66.3°C to 68.7°C), whereas peak temperature at 5 mm was different among five doses. Peak temperature at 5 mm was highest in the low power-long duration dose (61.1°C), followed by the mid-low power-mid duration dose (58.8°C) and mid-high power-short duration dose (55.0°C), and lowest in the mid power-short duration dose (52.0°C) and high power-ultra short duration dose (51.8°C).

IN VIVO STUDY

All fifteen animals survived the expected in-life phase of the study. One renal artery in the mid power and short duration group was excluded from histological analysis, since two emission sites could

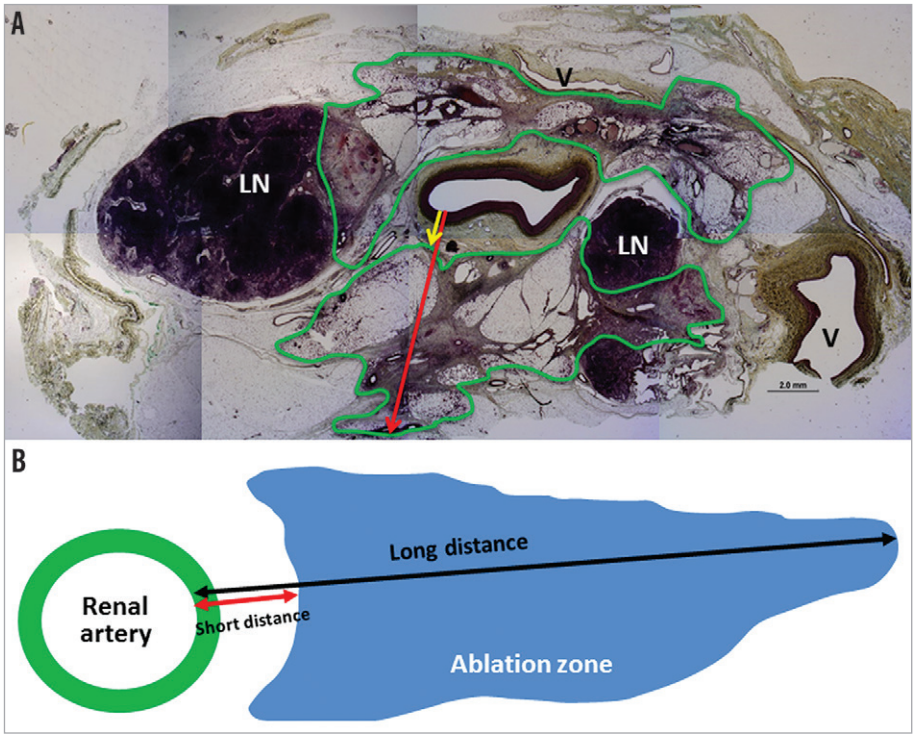

Figure 3. *Representative images of ablation area mapping. A) Representative histologic section of emission site. The ablation area is delineated by a green line. The red arrow represents maximum long distance, whereas the yellow arrow represents corresponding short distance. B) Diagram of area mapping and distance measurement. LN: lymph node ; V: vein.*

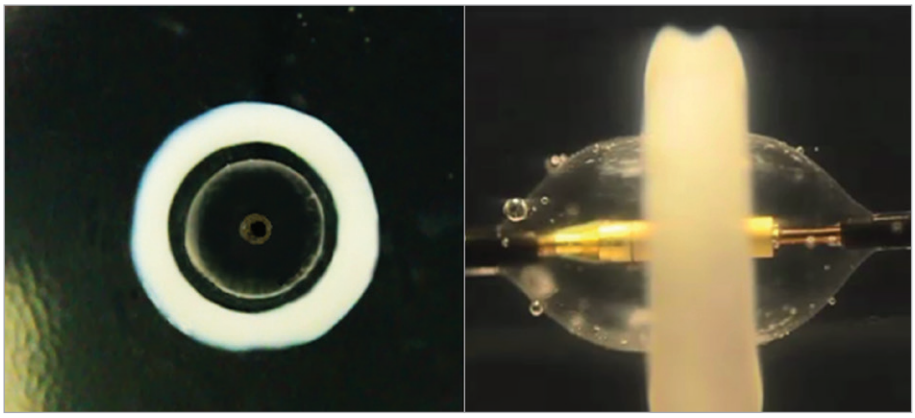

Figure 4. *Thermal gel model. The heating pattern generated by ultrasound energy delivered from the Paradise catheter is illustrated. The heat lesion is circumferential, uniform, and toroidal in shape, with a preserved cooled region adjacent to the balloon.*

Table 1. Near (1 mm) and far (5 mm) sensor temperature among 5 different doses.

	Low power-long duration	Mid-low power-mid duration	Mid power-short duration	Mid-high power-short duration	High power-ultra short duration
Peak temperature at 1 mm	66.9	68.7	67.0	67.2	66.3
Peak temperature at 5 mm	61.1	58.8	52.0	55.0	51.8

not be identified due to a short renal artery. A total of 29 RAs were used for analysis. The mean lengths of the renal artery from ostium to bifurcation in the low power-long duration group, mid-low power-mid duration group, mid power-short duration group, mid-high power-short duration group, and high power-ultra short duration group were 3.3±0.7 cm, 3.2±0.9 cm, 3.6±0.9 cm, 3.7±0.5 cm, and 3.4±1.1 cm, respectively (p=0.84). There was no balloon-related dissection observed in any of the arteries.

TOTAL ABLATION AREA AND DISTANCE

Table 2 shows the total ablation area, and the maximum and minimum distance among the five groups. The total ablation area was significantly greater in the low power-long duration group (172±70 mm^2), followed by the mid power-mid duration group (133±31 mm^2), and it was least in the mid power-short duration group (87±54 mm^2), the mid-high power-short duration group (87±11 mm^2), and the high power-ultra short duration group (85±32 mm^2) (p=0.02). The maximum distance was significantly longer in the low power-long duration group (11.9±2.9 mm), followed by the mid-low power-mid duration group (10.0±1.5 mm), the mid-high power-short duration group (10.2±2.3 mm), and the high power-ultra short duration group (10.1±1.3 mm), and it was shortest in the mid power-short duration group (7.4±2.0 mm) (p=0.007). On the other hand, minimum distance was not different among the five groups, ranging from 1.0±0.5 mm to 1.4±0.2 mm (p=0.38).

RENAL ARTERY, PERIARTERIAL SOFT TISSUE, AND NERVE INJURY

Table 3 shows renal artery, vein, arterioles, and soft tissue injury among the five groups. Endothelial loss was not observed in any group. Medial injury was minimal (score <1) both in depth and circumference, and was not different among the five groups (p=0.13). The number of injured tissue quadrants was similar among the five groups (p=0.79): all groups showed ≥3 quadrants of injured tissue, which supports circumferential energy emission. Other parameters including vein injury and arterioles injury were not different among the groups.

Table 4 shows nerve damage among the five groups. Nerve damage was similar among the five groups (p=0.73), and all groups showed marked (score 4) nerve damage. Injured nerve quadrant (score ≥2) per nerve quadrant, which reflects circumferential nerve damage,

Table 2. Total ablation area, maximum and minimum ablation distance among 5 different doses.

	Low power-long duration (n=6)	Mid-low power-mid duration (n=6)	Mid power-short duration (n=9)	Mid-high power-short duration (n=4)	High power-ultra short duration (n=4)	*p*-value
Total ablation area (mm^2)	172±70	133±31	87±54	87±11	85±32	0.02
Maximum distance (mm)	11.9±2.9	10.0±1.5	7.4±2.0	10.2±2.3	10.1±1.3	0.007
Minimum distance (mm)	1.2±0.3	1.4±0.2	1.2±0.4	1.0±0.7	1.1±0.4	0.50
p-value was calculated from one-way ANOVA test.						

Table 3. Renal artery, vein, arterioles, and soft tissue injury among 5 different doses.

		Low power-long duration (n=6)	Mid-low power-mid duration (n=6)	Mid power-short duration (n=9)	Mid-high power-short duration (n=4)	High power-ultra short duration (n=4)	*p*-value
Renal artery	Endothelium loss (score 0-4)	0±0	0±0	0±0	0±0	0±0	–
	Medial injury depth (score 0-4)	0±0	0±0	0.3±0.5	0.8±1.0	0.3±0.3	0.13
	Medial injury circumference (score 0-4)	0±0	0±0	0.2±0.3	0.5±0.7	0.3±0.3	0.13
Vein	Endothelium loss (0-4)	0±0	0.3±0.3	0.1±0.3	0±0	0±0	0.09
	Medial injury depth (score 0-4)	0±0	1.9±1.7	0.7±1.0	1.5±1.9	1.0±2.0	0.18
	Medial injury circumference (score 0-4)	0±0	0.6±0.5	0.3±0.4	0.4±0.5	0.3±0.5	0.20
Arterioles injury (score 0-4)		3.8±0.4	4.0±0	3.9±0.3	4.0±0	4.0±0	0.72
Number of injured tissue quadrants (0-4 quadrant)		3.2±0.8	3.4±0.4	3.2±0.7	3.1±0.9	3.0±0.4	0.79

p-value was calculated from Kruskal-Wallis test.

was not different among the five groups (p=0.10). Also, moderately to severely injured nerve quadrant (score ≥3) per nerve quadrant was not different among the five groups. Representative images of the emission site among the five groups are shown in **Figure 5**.

Overall retroperitoneal organ damage, consisting of focal psoas muscle necrosis, small bowel transmural necrosis and injury to the ureter, was observed **(Online Table 1)**, mostly in the low power-long duration, and mid-low power-mid duration groups, and the least injury was observed in the mid power-short duration group which coincides with the shortest ablation distance of perirenal soft tissue damage.

Discussion

This study aimed to assess the ability to modify the ablation geometry by changing ultrasound energy and duration while maintaining the safety of the arterial wall and the efficacy of nerve injury. Five ultrasound doses were evaluated in a thermal gel model and in an *in vivo* porcine model. The data demonstrated that the total ablation area as well as the maximum ablation distance from the arterial lumen can be controlled by varying the ultrasound dose (power and duration). The total ablation area and maximum distance were greatest in the low power-long duration group and least in the mid power-short duration group, which coincides with the results of the peak temperature at 5 mm in the gel model. The data further demonstrated that the minimum distance from the arterial lumen was similarly controlled, as the distance was not different among the five groups evaluated in either the thermal gel model or the *in vivo* porcine model. These results suggest that the mid power-short duration group showed the safest profile without sacrificing efficacy, because the maximum ablation distance (7.4±2.0 mm) in this group may be enough for human renal nerve ablation, at which the 90th percentile of all nerve distance was 6.39 mm[11]. The renal arterial wall exhibited minimal damage in all groups. There was no evidence of endothelial cell loss, and minimal to no medial damage. The minimal medial damage that was observed is not physiologically relevant. Marked circumferential grade 4 nerve damage was observed in all groups. The results of injured nerve quadrant per nerve quadrant were consistent with circumferential nerve damage. Furthermore, the mean number of injured tissue quadrants was ≥3 in all groups, which also suggests circumferential ablation geometry.

To date, there are few reports in the literature regarding catheter-based ultrasound renal denervation in preclinical models except reports of meeting abstracts. Koruth et al presented an abstract of catheter-based ultrasound renal denervation in adult swine[12]. They reported on acute (<30 hours) histopathologic changes induced by catheter-based ultrasound ablation, and observed that 86% of all nerves showed mild to complete nerve injury while inducing minimal arterial injury[12]. Recently, Wang et al reported their findings following renal denervation by extracorporeal high-intensity focused ultrasound in a canine model[13]. Although they reported the histology of nerve damage including vacuolisation, the detail of the ablation geometry (depth or circumference) was not described[13]. As compared to ultrasound denervation, RF energy-induced

Table 4. Nerve damage among 5 different doses.

	Low power-long duration (n=6)	Mid-low power-mid duration (n=6)	Mid power-short duration (n=9)	Mid-high power-short duration (n=4)	High power-ultra short duration (n=4)	*p*-value
Nerve injury (score 0-4)	3.9±0.2	3.8±0.4	3.7±0.5	3.9±0.3	4.0±0	0.73
Injured nerve quadrant (score ≥2) per nerve quadrant	0.7±0.1	0.9±0.1	0.8±0.2	0.8±0.1	0.9±0.2	0.10
Injured nerve quadrant (score ≥3) per nerve quadrant	0.6±0.1	0.8±0.3	0.7±0.3	0.7±0.2	0.8±0.2	0.23

p-value was calculated from Kruskal-Wallis test.

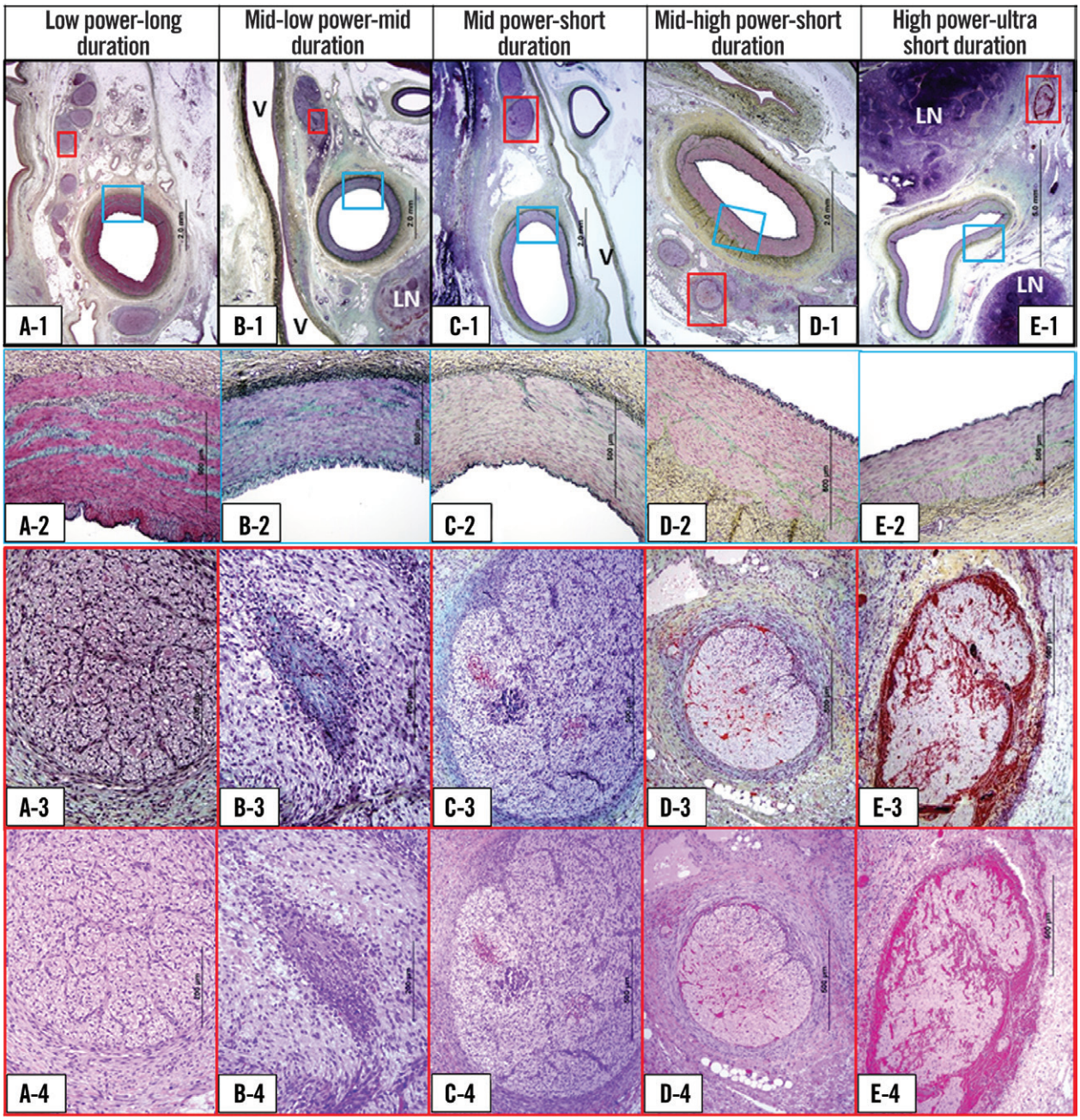

Figure 5. *Representative histologic images of emission site among 5 different dose groups. Panel A. Low power-long duration. A-1: low magnification images of renal artery and surrounding tissue (Movat stain). A-2: high magnification image of arterial media (blue boxed area in A-1). Arterial media is intact (Movat stain). A-3 and A-4: high magnification image of injured nerve fascicle (red boxed area in A-1). Moderate (Grade 3) nerve injury is observed (A-3: Movat stain, A-4: H&E stain). Panel B. Mid-low power-mid duration. B-1: low magnification images of renal artery and surrounding tissue (Movat stain). V: vein; LN: lymph node. B-2: high magnification image of arterial media (blue boxed area in B-1). Arterial media is intact (Movat stain). B-3 and B-4: high magnification image of injured nerve fascicle (red boxed area in B-1). Severe (Grade 4) nerve injury is observed (B-3: Movat stain, B-4: H&E stain). Panel C. Mid power-short duration. C-1: low magnification images of renal artery and surrounding tissue (Movat stain). V: vein. C-2: high magnification image of arterial media (blue boxed area in C-1). Arterial media is intact (Movat stain). C-3 and C-4: high magnification image of injured nerve fascicle (red boxed area in C-1). Severe (Grade 4) nerve injury is observed (C-3: Movat stain, C-4: H&E stain). Panel D. Mid-high power-short duration. D-1: low magnification images of renal artery and surrounding tissue (Movat stain). D-2: high magnification image of arterial media (blue boxed area in D-1). Arterial media is intact (Movat stain). D-3 and D-4: high magnification image of injured nerve fascicle (red boxed area in D-1). Severe (Grade 4) nerve injury is observed (D-3: Movat stain, D-4: H&E stain). Panel E. High power-ultra short duration. E-1: low magnification images of renal artery and surrounding tissue (Movat stain). LN: lymph node. E-2: high magnification image of arterial media (blue boxed area in E-1). Arterial media is intact (Movat stain). E-3 and E-4: high magnification image of injured nerve fascicle (red boxed area in E-1). Severe (Grade 4) nerve injury is observed (E-3: Movat stain, E-4: H&E stain).*

preclinical studies of renal denervation have been reported in two separate studies by Rippy et al and Steigerwald et al[14,15]. However, information regarding RF ablation geometry was not reported except for mentioning the presence of nerve damage observed at three different time points (six months by Rippy et al, and 45 min and 10 days by Steigerwald et al) by these two investigators.

In catheter-based renal sympathetic denervation, it is of utmost importance to control the ablation geometry in order to maintain the efficacy and safety. Ideally, the maximum ablation distance should be long enough to affect most of the perirenal nerves[11] but should not be too deep as to cause excessive deep ablation that could jeopardise periarterial organs. The present study demonstrated that the target ablation area and maximum depth can be controlled with the ultrasound Paradise System, while the cooling balloon feature consistently spares the first mm of tissue (arterial wall) from injury. Although retroperitoneal organ damage such as focal psoas muscle and small intestine necrosis were observed in the current study, the distance from renal artery to those organs is anatomically different in pigs as compared to in man. The distance from the renal artery to psoas muscle is greater in man than in swine (unpublished CT data: ReCor Medical). Therefore, direct translation of our results to humans is probably not applicable.

Circumferential nerve ablation has the advantage of achieving adequate transection of the nerves; however, the primary risk of circumferential denervation is extensive arterial damage. The Paradise System maintains a cooled surface circumferentially to prevent arterial damage. The Paradise System delivered energy radially resulting in Grade 2 nerve injury to 70-90% of the nerves, and Grade 3 injury to 60-80% of the nerves. Nonetheless, it was not possible to ablate 100% of the nerves circumferentially due to the presence of areas of heat sink such as the lymph nodes and renal vein which, to some extent, are random, and the location of heat sink is not constant **(Figure 3)**.

Ultrasound ablation offers certain advantages over RF ablation for renal denervation due to the manner by which energy is generated and delivered to the tissue. The ability to induce thermal damage without the energy source needing to make direct contact with the arterial wall is one of the main distinctions between ultrasound and RF devices. RF devices require impedance measurements to ensure proper contact with tissue, a step that is unnecessary when ultrasound is used. Since direct tissue contact is necessary to ablate tissue with RF electrodes, the tissue receiving the highest influx of energy is immediately adjacent to the electrode. In contrast, ultrasound devices do not require direct tissue contact, and balloon cooling of the arterial wall can be implemented while maintaining stabilisation and position of the device within the artery. Balloon cooling allows for the maintenance of physiologic temperatures in the tissue in immediate contact with the balloon. Another important distinction is that RF relies on thermal conduction alone to denervate nerves residing away from the arterial wall.

Although both the Paradise System and the RF denervation system have been used in many different patient populations, all have shown the safety of these devices in clinical trials. However, effectiveness has been questioned lately (SYMPLICITY HTN-3[16]). Greater understanding of each device in preclinical studies is needed and their effectiveness will have to be proven in future randomised trials. At least in the current study we have shown that ultrasound energy delivered via the Paradise System in the porcine model can result in sparing of the renal artery while inducing greater perirenal tissue and nerve damage. However, no head-to-head comparison to RF ablation was performed.

Study limitations

While clear morphological nerve damage was observed in all groups, functional nerve damage, such as immunohistochemistry, was not evaluated, and norepinephrine levels in the kidney were not measured in this study. We showed maximum distance as well as corresponding shortest distance; however, these results may be affected by tissue shrinkage due to histological processing and therefore the measurement may not exactly correspond to the *in vivo* situation[17]. Also, since some histologic sections did not have uninvolved edge, the maximum depth may have been underestimated. Furthermore, clinical implications of preclinical findings are always uncertain due to differences in anatomy and the use of non-diseased models. However, there are no reliable immediate biomarkers to assess the success or failure of in-human renal sympathetic denervation. Preclinical histopathologic studies are the only means of determining the extent of nerve damage, which is as yet impossible in the clinical setting. In addition, the failure to reach efficacy endpoint in the SYMPLICITY HTN-3 trial underscores the importance of preclinical work in this field[16].

Conclusions

The Paradise® Ultrasound Renal Denervation System can modify total ablation area and depth by changing ultrasound power and duration while maintaining renal arterial safety and sufficient periarterial nerve damage.

Impact on daily practice

In catheter-based renal sympathetic denervation, it is of the utmost importance to control the ablation geometry in order to maintain the efficacy and safety. Ideally, the maximum ablation distance should be long enough to affect most of the perirenal nerves but should not be too deep as to cause excessive deep ablation that could jeopardise periarterial organs. The present preclinical study demonstrated that the target ablation area and maximum depth can be controlled with the ultrasound Paradise System. Although clinical implications of preclinical findings are always uncertain due to differences in anatomy and the use of non-diseased models, preclinical histopathologic studies are the only means of determining the extent of nerve damage, which is impossible in the clinical setting.

Acknowledgements

The authors would like to thank ISIS Services, LLC, for excellent procedures in animal work.

Funding

This study was sponsored by ReCor Medical Inc. CVPath Institute Inc., a private non-profit research organisation, provided partial

support for this work. K. Sakakura is supported by a research fellowship from the Banyu Life Science Foundation.

Conflict of interest statement

K. Sakakura has received speaking honoraria from Abbott Vascular, Boston Scientific, and Medtronic CardioVascular. A. Roth and L. Coleman are employees of ReCor Medical. M. Joner is a consultant for Biotronik and Cardionovum, and has received speaking honoraria from Abbott Vascular, Biotronik, Cordis J&J, Medtronic and St. Jude. R. Virmani receives research support from 480 Biomedical, Abbott Vascular, Atrium, Biosensors International, Biotronik, Boston Scientific, Cordis J&J, GSK, Kona, Medtronic, MicroPort Medical, OrbusNeich Medical, ReCor Medical, SINO Medical Technology, Terumo Corporation, and W.L. Gore. He has speaking engagements with Merck. He receives honoraria from 480 Biomedical, Abbott Vascular, Biosensors International, Boston Scientific, CeloNova BioSciences, Claret Medical, Cordis J&J, Lutonix Bard, Medtronic, ReCor Medical, Terumo Corporation, and W.L. Gore, and is a consultant for 480 Biomedical, Abbott Vascular, Medtronic, and W.L. Gore. The other authors have no conflicts of interest to declare.

References

1. James PA, Oparil S, Carter BL, Cushman WC, Dennison-Himmelfarb C, Handler J, Lackland DT, Lefevre ML, Mackenzie TD, Ogedegbe O, Smith SC Jr, Svetkey LP, Taler SJ, Townsend RR, Wright JT Jr, Narva AS, Ortiz E. 2014 evidence-based guideline for the management of high blood pressure in adults: report from the panel members appointed to the Eighth Joint National Committee (JNC 8). *JAMA.* 2014;311:507-20.

2. Calhoun DA, Jones D, Textor S, Goff DC, Murphy TP, Toto RD, White A, Cushman WC, White W, Sica D, Ferdinand K, Giles TD, Falkner B, Carey RM. Resistant hypertension: diagnosis, evaluation, and treatment. A scientific statement from the American Heart Association Professional Education Committee of the Council for High Blood Pressure Research. *Hypertension.* 2008;51:1403-19.

3. Mancia G, Grassi G, Giannattasio C, Seravalle G. Sympathetic activation in the pathogenesis of hypertension and progression of organ damage. *Hypertension.* 1999;34:724-8.

4. Schlaich MP, Schmieder RE, Bakris G, Blankestijn PJ, Bohm M, Campese VM, Francis DP, Grassi G, Hering D, Katholi R, Kjeldsen S, Krum H, Mahfoud F, Mancia G, Messerli FH, Narkiewicz K, Parati G, Rocha-Singh KJ, Ruilope LM, Rump LC, Sica DA, Sobotka PA, Tsioufis C, Vonend O, Weber MA, Williams B, Zeller T, Esler MD. International expert consensus statement: Percutaneous transluminal renal denervation for the treatment of resistant hypertension. *J Am Coll Cardiol.* 2013;62:2031-45.

5. Mahfoud F, Ewen S, Ukena C, Linz D, Sobotka PA, Cremers B, Bohm M. Expanding the indication spectrum: renal denervation in diabetes. *EuroIntervention.* 2013;9:R117-21.

6. Bohm M, Ewen S, Kindermann I, Linz D, Ukena C, Mahfoud F. Renal denervation and heart failure. *Eur J Heart Fail.* 2014;16:608-13.

7. Esler MD, Krum H, Sobotka PA, Schlaich MP, Schmieder RE, Bohm M. Renal sympathetic denervation in patients with treatment-resistant hypertension (The Symplicity HTN-2 Trial): a randomised controlled trial. *Lancet.* 2010;376:1903-9.

8. Mabin T, Sapoval M, Cabane V, Stemmett J, Iyer M. First experience with endovascular ultrasound renal denervation for the treatment of resistant hypertension. *EuroIntervention.* 2012;8:57-61.

9. National Research Council. Guide for the Care and Use of Laboratory Animals, 8th Edition. Washington, DC, USA: National Academies Press; 2011.

10. Sakakura K, Ladich E, Edelman ER, Markham P, Stanley JR, Keating J, Kolodgie FD, Virmani R, Joner M. Methodological Standardization for the Pre-Clinical Evaluation of Renal Sympathetic Denervation. *JACC Cardiovasc Interv.* 2014 Sep 9. [Epub ahead of print].

11. Sakakura K, Ladich E, Cheng Q, Otsuka F, Yahagi K, Fowler D, Kolodgie F, Virmani R, Joner M. Anatomical assessment of sympathetic peri-arterial renal nerves in man. *J Am Coll Cardiol.* 2014;64:635-43.

12. Koruth J, Dukkipati S, Miller M, Sinelnikov Y, Zou Y, Smith D, d'Avila A, Reddy VY. Selective Renal Sympathetic Denervation With Arterial Sparing?: An in vivo Proof of Principle Study Using Ultrasound Energy (Abstract). *Circulation*. 2011;124:A16042.

13. Wang Q, Guo R, Rong S, Yang G, Zhu Q, Jiang Y, Deng C, Liu D, Zhou Q, Wu Q, Wang S, Qian J, Wang Q, Lei H, He TC, Wang Z, Huang J. Noninvasive renal sympathetic denervation by extracorporeal high-intensity focused ultrasound in a preclinical canine model. *J Am Coll Cardiol.* 2013;61:2185-92.

14. Rippy MK, Zarins D, Barman NC, Wu A, Duncan KL, Zarins CK. Catheter-based renal sympathetic denervation: chronic preclinical evidence for renal artery safety. *Clin Res Cardiol.* 2011;100:1095-101.

15. Steigerwald K, Titova A, Malle C, Kennerknecht E, Jilek C, Hausleiter J, Nahrig JM, Laugwitz KL, Joner M. Morphological assessment of renal arteries after radiofrequency catheter-based sympathetic denervation in a porcine model. *J Hypertens.* 2012;30:2230-9.

16. Bhatt DL, Kandzari DE, O'Neill WW, D'Agostino R, Flack JM, Katzen BT, Leon MB, Liu M, Mauri L, Negoita M, Cohen SA, Oparil S, Rocha-Singh K, Townsend RR, Bakris GL; SYMPLICITY HTN-3 Investigators. A controlled trial of renal denervation for resistant hypertension. *N Engl J Med.* 2014;370:1393-401.

17. Virmani R, Avolio AP, Mergner WJ, Robinowitz M, Herderick EE, Cornhill JF, Guo SY, Liu TH, Ou DY, O'Rourke M. Effect of aging on aortic morphology in populations with high and low prevalence of hypertension and atherosclerosis. Comparison between occidental and Chinese communities. *Am J Pathol.* 1991;139:1119-29.

Online data supplement

Online Table 1. Summary of organ findings.